An Investigation of Distance Protection Function Applied for Shunt Reactors

M. L. S. Almeida, K. M. Silva

***Abstract*—This article investigates the use of the distance function to protect shunt reactors. For this purpose, mho phase comparator is assessed. To carry out a comparative evaluation, the distance function performance was further compared with the differential function performance. Moreover, the Alternative Transit Program (ATP) was applied to model an electrical system, in which the reactor is subjected to different faults, including phase-to-phase, phase-to-ground, turn-to-ground and turn-to-turn faults. The performance of the evaluated distance function was also investigated against the number of turns involved and the leakage factor. From the results obtained, it is suggested the joint use of the distance function with the differential protection, because if the differential function does not operate, distance function would guarantee the operation for internal faults, including turn-to-ground and turn-to-turn faults, increasing reliability of protection scheme for shunt reactors. Also, the present study may serve as a guide for further studies, for example, that evaluate the use of distance function to protect iron-core reactors.**

***Keywords*—Distance protection, mho phase comparator, shunt reactor, turn-to-ground faults and turn-to-turn faults.**

I. Introduction

SHUNT reactors are equipment used in long-distance, high-voltage power transmission lines to ensure the reactive power control of the line. When the system operates with light load, there is an excess of reactive power on the line that can cause overvoltages, which are harmful to the equipment connected to the electrical system. Under these conditions, the reactors are connected in parallel with the line, in order to absorb excess reactive power, allowing the line to operate within adequate voltage rate. Therefore, ensuring safe operation conditions for shunt reactors is fundamental for the correct functioning of transmission system.

To identify abnormal operating conditions of the reactors, differential protection is normally used, by means of phase elements [1] and also by means of the restricted earth fault (REF) function [2]. The performance of differential function for shunt reactor is safer when there are faults with high fault current, such as faults 1 and 2, shown in Fig. 1, that represents one solidly grounded reactor circuit, where SCP is the system connection point. In fault 1 (corresponding to a phase-to-ground fault) and in fault 2 (representing a phase-to-phase fault), the fault current is high, since the whole winding is involved [3].

It should be noted that due to reactor construction, there is a secure space between the phases, which results in better isolation between them, such that faults 3 are rare [4]. Fault 3 corresponding to phase-to-phase faults with a percentage of the winding of faulted phases short-circuited. Even so, as the fault occurs between two distinct phases, the current after the fault is high, such that the differential function is able to operate.

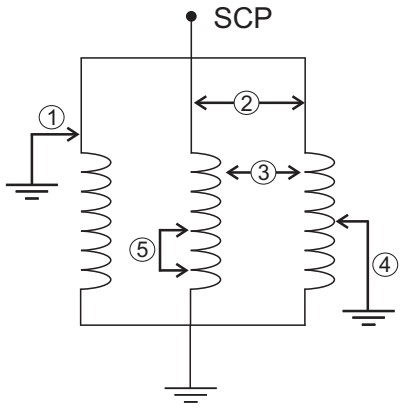

Fig. 1. Faults in shunt reactor.

In Fig. 1, faults 4 correspond to turn-to-ground faults and are also identified by differential functions whenever they take a large number of turns. Nevertheless, if this type of fault takes a smaller number of turns or it has a high fault resistance, the differential functions are not able to operate, since the fault currents have low values, which may be lower than the pick up setting of the differential function [5]. The challenge is even greater for the identification of faults 5 in Fig. 1, called turn-to-turn faults, because even with the occurrence of the fault, the currents in shunt reactor experience minimal changes, causing the currents to present practically the same value as before the fault.

To identify turn-to-ground and turn-to-turn faults with few turns involved, a differential function based on an alpha plane, which compares the zero sequence current and the neutral current of the reactor, was proposed in [6]. According to the obtained results, the proposed logic operate correctly for all simulated faults, including critical ones with large value of leakage factor, few turns involved and high fault resistance. A comparison between the logic presented in [6] and the one proposed by [7], which is also a differential function, but based on the generalized alpha plane, was presented in [8].

In addition to the differential function, some authors also propose the use of distance protection for reactors [9], [10]. According to [11], distance protection can be combined with differential and overcurrent protection to identify faults

Financial support should be acknowledged here. Example: This work was supported in part by the U.S. Department of Commerce under Grant BS123.

Paper submitted to the International Conference on Power Systems Transients (IPST2023) in Thessaloniki, Greece, June 12-15, 2023.

with high magnitude. To identify turn-to-turn faults in shunt reactors, [5] proposes the use of distance protection, since it can identify the significant reduction of the shunt reactor impedance, during turn-to-turn faults. However, according to [12], when used to protect reactors, the distance protection can present unstable behavior during switching.

Considering the possibility of using distance function for shunt reactors, the objective of this article is to present a detailed study on the use of the distance function to protect dry-type reactors. It should be noted that in the relevant literature there are few references that describe in detail this application. More specifically, it appears that there is no reference that assesses the influence of the leakage factor and the number of short-circuited turns on the performance of the distance function. Thus, this article also aims to present a detailed study that investigates the influence of these parameters on the performance of distance protection function. Therefore, the present study may serve as a guide for further studies, for example, that evaluate the use of distance function to protect iron-core reactors.

In short, the focus of this work is to investigate the distance protection function, so that the differential function is presented as a reference. To do so, a comparative evaluation is developed, such that the performance of distance function was compared with the one of differential function, through the analysis of the tripping times. Moreover, as the traditional differential function does not operate for faults with low fault currents, for these cases it was decided to compare the performance of distance function with the performance of an alternative differential function, based on the adapted alpha plane.

In this context, aiming to evaluate critical internal fault situations, different faults were simulated, as phase-to-ground and phase-to-phase faults. Furthermore, turn-to-ground and turn-to-turn faults were also evaluated, by varying the number of turns involved and the value of leakage factor. It is noteworthy that for this implementation, mho phase comparators are evaluated, as it has been widespread used [13]. To do so, the Alternative Transient Program (ATP) software was used to model an electric power system composed of a 500 kV/60 Hz line 400 km long with 60% shunt compensation through dry-type air-core shunt reactors. Moreover, the performance of the distance function will be compared with the differential function based on the phase elements and the differential function presented in [6].

II. Distance Function Protection

Based on current and voltage values, measured through current transforms (CT) and potential transformers (PT), respectively, distance function calculates the impedance units, which are evaluated to determine distance function trip. These units are calculated using Phase-to-Ground and Phase-to-Phase elements, such that they operate according to the characteristics of the fault [13].

For the implementation of distance protection, the impedance units can still be interpreted by means of phase and magnitude comparators, which are quite used. The operation of these comparators is carried out by two signals, which are compared and from their phase difference, or the relationship between their magnitudes, it is possible to distinguish between a normal system operation situation and the occurrence of a fault [14]. The presented article uses the mho characteristic, that is widely used in distance relays due to its finite range, directionality, simplicity (implemented by only one comparator), good accommodation of the fault resistance and less sensitivity to power fluctuations [13]. It is noteworthy that the equation described below is implemented in an analogous way to what is traditionally done for transmission lines, but considering the application for a shunt reactor.

It should be noted that in situations of faults whose voltage value goes to zero, the distance function could operate incorrectly due to losing its reference signal. To solve this problem, voltage polarization strategies are usually employed, and in this article, it was considered the positive sequence voltage memory filter, described in [15]. This strategy shows better behavior against all types of faults, even those with voltages close to zero or with inversion voltage on compensated lines. In this way, based on phases voltages and through Fortescue matrix, the positive sequence voltage phasor ($\widehat{V}_1$) is calculated as the input of the filter, which output is the memorized version $\widehat{V}_{1m}$, as described in 1.

$$\widehat{V}_{1m}(k) = \alpha\widehat{V}_1(k) + (1-\alpha)\,\widehat{V}_{1m}(k-1)\ , \tag{1}$$

where k represents the k-th sampling instant and α is the vanishing factor. Thus, based on $\widehat{V}_{1m}$ and on the phase sequence considered, the memorized voltage on phase ϕ ($\widehat{V}_{m\phi}$) are determined, where ϕ represents phases A, B or C.

Considering the use of the positive sequence voltage memory filter and according to [16], for the distance function to be interpreted as a phase comparator with mho characteristic, the phasor of the operating voltage ($\widehat{V}_{op\phi}$) and the polarization voltage ($\widehat{V}_{pol\phi}$) must be defined respectively as described in (2) and (3).

$$\widehat{V}_{op\phi}(k) = -\widehat{V}_{\phi}(k) + \frac{hZ_R}{\cos(\theta_{Z_R} - \tau)}\widehat{I}_{\phi}(k) \tag{2}$$

$$\widehat{V}_{pol\phi}(k) = \widehat{V}_{m\phi}(k) \tag{3}$$

where $\widehat{V}_{\phi}$ is the voltage phasor on phase ϕ; $\widehat{I}_{\phi}$ is the current phasor measured on the terminal of phase ϕ; h is the percentage to be protected of the total shunt reactor impedance; Z_R is the reactor impedance; θ_{Z_R} is the angle of Z_R; τ is the project angle of the mho characteristic, or maximum torque angle of the relay. It should be noted that the fraction that multiplies $\widehat{I}_{\phi}$ is defined as Z_A and corresponds to the relay range impedance.

The output angle of the phase comparator, wich is determined as the phase difference between $\widehat{V}_{op\phi}$ and $\widehat{V}_{pol\phi}$ (called θ_{ϕ}), must issue a trip if is less than $90°$, otherwise its operation should be restrained [16].

The operating voltage and the polarization voltage of the phase comparator for the mho characteristic can be also interpreted as impedances. To do so, the equations (2) and 3 must be divided by $\widehat{I}_{\phi}$, which results in operation impedance

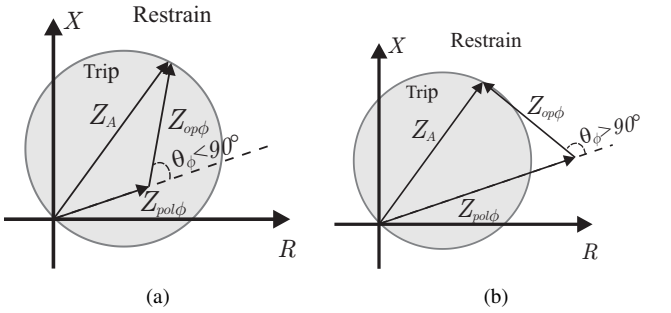

Fig. 2. Relationship between the phases of $Z_{op\phi}$ and $Z_{pol\phi}$: (a) within the mho characteristic; (b) outside the mho characteristic.

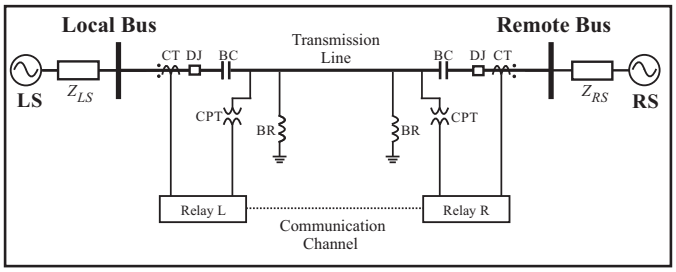

Fig. 3. Single line diagram of the evaluated power system model.

($Z_{op\phi}$) and polarization impedance ($Z_{pol\phi}$). From Fig. 2 it can be seen when $Z_{op\phi}$ and $Z_{pol\phi}$ are plotted in the R-X plane, in which two situations can be observed: inside the mho characteristic (Fig. 2(a)) and out of mho characteristic (Fig. 2(b)). In the first case the condition $\theta_\phi < 90°$ is satisfied, so that the relay detects the fault within its operating characteristic. In the second case $\theta_\phi > 90°$, so that the relay does not operate.

It should be noted that during normal operating conditions, the ratio between the voltage at the reactor terminals and the current through the reactor results exactly in the value of the reactor impedance. Therefore, to prevent distance function from operating incorrectly during normal operating conditions, in this article the value of $h = 0.9$ has been adjusted. Furthermore, τ was determined to be equal to the reactor impedance angle in order to ensure the maximum torque angle of the relay.

III. Presentation of Results

The assessment of distance function application for shunt reactors was carried out considering simulations developed in the ATP, in which different fault simulations of phase-to-ground, phase-to-phase, turn-to-ground and turn-to-turn faults were evaluated. For this purpose, an electric power system was modeled as shown in Fig. 3, composed by a 500 kV/60 Hz line 400 km long with 60 % shunt compensation by means of dry-type air-core shunt reactors. These reactors are installed at both line ends and each of them has the impedance of $40 + j1718.86\ \Omega$.

To do so, all faults indicated in Fig. 1 were be simulated. In the present article, the transient analysis of faults conditions that lead to largest fault currents was carried out. As discussed earlier, phase-to-ground and phase-to-phase faults (corresponding to faults 1 and 2, respectively, in Fig. 1) are applied at phase terminals, such that the entire winding is short-circuited. Consequently, these faults result in high fault currents, and thus they are evaluated in the transient analysis. The choice to analyze the phase-to-phase faults with a percentage of the winding of faulted phases short-circuited (corresponding to the fault 3 in Fig. 1) in the transient simulations was basically because faults 3 result in high fault currents, as winding of different phases are short-circuited.

On the other hand, it was decided to evaluate the fault situations that result in low fault currents in the parametric sensitivity analysis. In this type of simulation it is possible to visualize graphically in a clearer and more concise way how the protection function is sensitive to the number of short-circuited turns and the value of the leakage factor. Therefore, as the turn-to-ground and turn-to-turn faults (corresponding to faults 4 and 5, respectively, in Fig. 1) normally result in low fault currents, mainly in situations with few turns involved and with a high value of leakage factor, they are evaluated in parametric sensitivity analysis.

Firstly, the simulations were evaluated during time in the transient analysis, in order to assess the performance of distance protection function (θ_ϕ) during transients. To carry out a comparative evaluation, for the evaluated internal faults, the performance of the differential protection function based on the phase elements (implemented as described in [16]) was also presented.

Then the parametric sensitivity analysis were performed, in which the behavior of distance function during the fault steady-state regime are evaluated. As the differential function based on phase elements fails to detect these faults [5], the performance of differential algorithm proposed in [6] was analyzed in the parametric sensitivity analysis, aiming to present a comparative evaluation with the distance function.

A. Transient Analysis

The characteristics of cases simulated in the transient analysis are described in Tab. I. Furthermore, to carry out a comparative evaluation, the performance of phase differential elements are also presented. According to [16], for the phase differential elements, the currents measured at phase terminal and neutral point are used to calculate the operating current (I_{op}) and the restraining current (I_{res}). The trip occurs when the two conditions described in 4 are fulfilled, where I_{pk} is the pick-up current and SLP is a factor to adjust the protection sensibility. In this paper, it is considered $I_{pk} = 0.1$ and $SLP = 0.6$, which are values typically employed.

$$I_{op} > SLP \cdot I_{res} \text{ e } I_{op} > I_{pk}. \quad (4)$$

Aiming to ensure protection security, the first situation evaluated is the energization maneuver of the shunt reactor, which corresponds to the Case 1 in Tab. I. From this analysis, Figs. 4 and 5 are presented, which correspond, respectively, to the waveforms of three-phase voltages and currents in the shunt reactor during the energization, which occurs in 100 ms.

From Fig. 4(a), it can be seen that waveforms of three-phase voltages are balanced from the beginning of the energization maneuver. To improve the visualization, a zoom between

TABLE I
FEATURES OF THE EVALUATED FAULTS FOR TRANSIENT ANALYSIS.

Case	Description
1	Shunt reactor energization
2	Phase-to-ground fault, evolving the entire winding of phase B
3	Phase-to-phase fault close to the phase terminals
4	Phase-to-phase fault with 80% of faulted phases short-circuited
5	Phase-to-phase fault with 20% of faulted phases short-circuited
6	Three-phase external fault
7	Phase-to-ground AT external fault

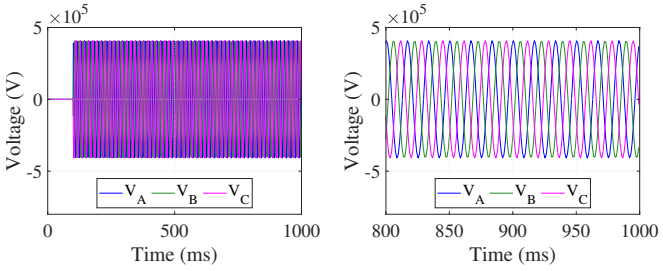

Fig. 4. Reactor voltage waveforms during energization: (a) from 100 ms until 1000 ms (b) from 800 ms until 1000 ms.

800 ms and 1000 ms is indicated in Fig. 4(b), in which it is clearly verified that the waveforms of three-phase voltages are balanced. From Fig. 5(a), one can observe that waveforms of three-phase currents start unbalanced right after energization, due to the transient generated by this maneuver. After that, waveforms of three-phase currents are also balanced, as shown in Fig. 5(b), which indicates the interval between 800 ms and 1000 ms.

The behavior of θ_ϕ during the energization maneuver are presented in Fig. 6(a). It can be seen that θ_ϕ oscillates in the beginning, but it remains on the restraining region, revealing the distance protection function avoids false trip during energization maneuvers. Likewise, from Fig. 6(b), it can be seen that the phase differential element also does not operate during the reactor energization.

The performance of the distance protection function for a phase-to-ground fault, evolving the entire winding of phase B, was evaluated in Case 2 described in Tab. I. It should be noted that this fault is the same of fault 1, shown in Fig. 1, and it was applied in 100 ms. From Fig. 7(a), it is observed that θ_B operates correctly, moving to the trip region 3 ms after the fault occurrence. It is noteworthy that for this case, only the faulted

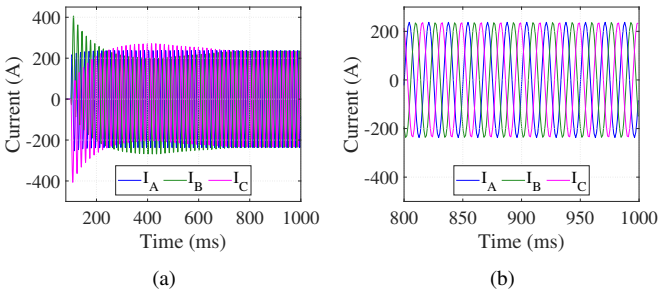

Fig. 5. Reactor currents waveforms during energization: (a) from 100 ms until 1000 ms (b) from 800 ms until 1000 ms.

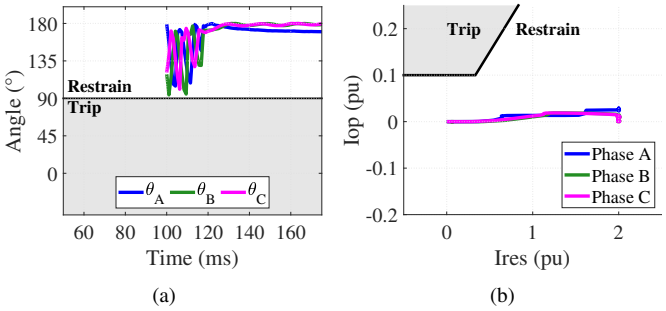

Fig. 6. The performance during energization of: (a) distance function (b) differential function.

phase element moved to the trip region, thus guaranteeing the correct selection of the faulted phase. Differential function performance for phase-to-ground fault is presented in Fig. 7(b). Since the phase-to-ground fault was applied in phase B, the phase B differential element moves to the trip region, with approximately 3 ms after the fault occurrence.

The Case 3 described in Tab. I corresponds to a phase-to-phase fault applied close to the phase terminals (similar to the fault 2 in Fig. 1). The results are presented in Fig. 8. In this case, the fault takes place at 100 ms and evolves the entire winding of phases B and C. From Fig. 8(a), it can be seen that θ_C shifts to trip region 3 ms after the fault occurrence, as seen in Fig. 8(a). Thus, the phase-to-phase fault is identified by at least one of the distance function indicators, which is sufficient to send a trip to the circuit breaker. Differential protection function performance for phase-to-phase fault close to the phase terminals is presented in Fig. 8(b). It is observed that the faulted phases (B and C) moved to the tripping region. Furthermore, one can see that the tripping time for this fault was approximately 3 ms after the fault occurrence.

It was also evaluated the fault 3 in Fig. 1, that corresponds to a phase-to-phase fault taking part of the winding of the faulted phases. For this analysis, the faults were applied in 100 ms and between phases B and C, and two situations were evaluated: both phases with 80% of their winding short-circuited (that corresponds to Case 4 of Table I and whose results are shown in Fig. 9) and both phases with 20% of winding short-circuited (that corresponds to Case 5 of Table I and whose results are presented in Fig.10). For these two cases, it is verified that θ_B and θ_C shift to the trip region, such that distance function operate, as can be seen from Figs. 9(a) and 10(a).

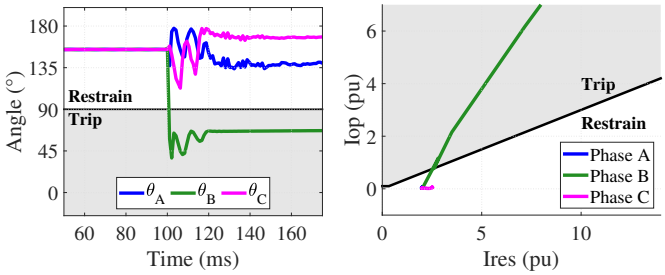

Fig. 7. The performance during a phase-to-ground fault of: (a) distance function (b) differential function.

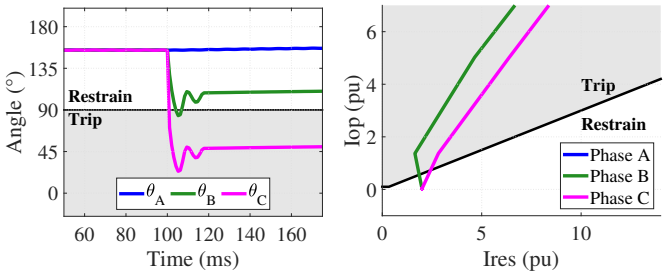

Fig. 8. The performance for a phase-to-phase fault (close to the phase terminals) of: (a) distance function (b) differential function.

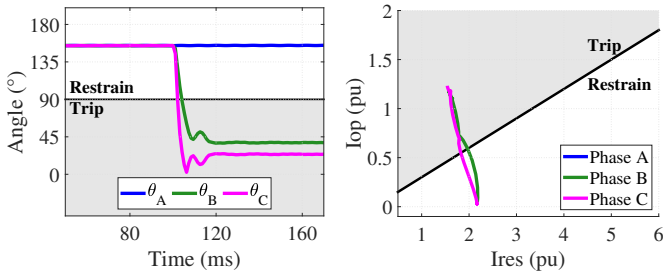

Fig. 10. The performance for a phase-to-phase fault with 20% of faulted phases short-circuited of: (a) distance function (b) differential function.

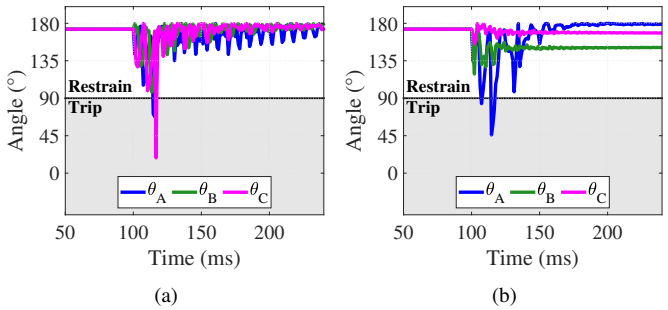

Fig. 11. The performance for a three-phase external fault: (a) distance function (b) differential function.

It is noteworthy that for Case 4 the tripping time was 4 ms, and for Case 5 the tripping time was 14 ms. The tripping time for Case 5 was longer, since the fault current is smaller, as a smaller amount of turns were short-circuited.

The performance of differential function for the last two cases of phase-to-phase fault evaluated, with 80% and 20% of faulted phases short-circuited were also investigated and their results are presented in Figs. 9(b) and 10(b), respectively. Since these faults evolves phases B and C, these faulted phases move to trip region for both cases, as indicated in Figs. 9(b) and 10(b). It should be noted that the tripping time for these two faults was approximately 3 ms after the fault occurrence.

Besides analyzing the performance of a protection function for internal faults, it is important to verify it does not operate for external faults. Thus, it should be noted that external faults close to the reactor, for example on the transmission line or on the local bus in Fig 3, would cause the line or local bus protection functions to trip, shutting down the reactor as consequence. Then, for the simulation of external faults,

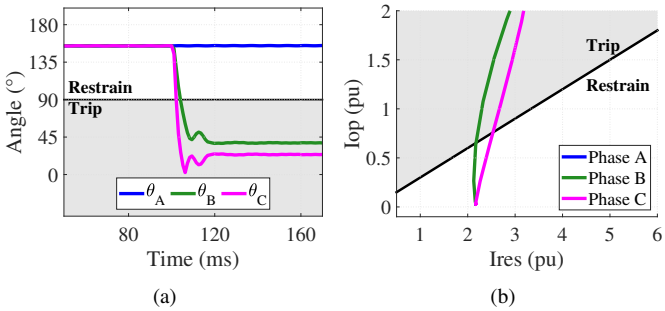

Fig. 9. The performance for a phase-to-phase fault with 80% of faulted phases short-circuited of: (a) distance function (b) differential function.

the system of Fig. 3 was changed in such a way that two equal transmission lines (each of them with 230 km and same parameters as the line in Fig. 3) were connected upstream of the local bus. On one of these lines, three-phase external fault and phase-to-ground AG external fault were simulated 5 km away from the local bus. Thus, these external faults were applied close to the reactor, but their occurrence should not lead the reactor protection function to operate.

In Figs. Figs. 11(a) and 11(b) are presented respectively the results for a three-phase external fault and a phase-to-ground AG external fault, that corresponds to Cases 6 and 7 of Table I. For these two external faults, the distance function did not operate immediately after the fault. However, θ_ϕ of the faulty phases presented oscillations, and falls in the operating region during a period of time, which could cause a false trip issuing. Note that after transients, θ_ϕ stabilizes in the restraining region. Therefore, it is suggested to reduce the reach of distance zone (reduction of the parameter h in equation 3), avoiding the distance protection malfunction during external faults.

B. Parametric Sensitivity Analysis

Parametric sensitivity analysis allows to evaluate the influence of a specific parameter on the performance of the protection function. Therefore, in order to assess the influence of the number of turns involved in the performance of the distance protection function, different cases of turn-to-ground and turn-to-turn faults (which correspond to faults 4 and 5, respectively, in Fig. 1) were simulated.

In order to simulate turn-to-ground and turn-to-turn faults, model proposed by [17] was considered. In this model, the mutual coupling formed during the fault between the

subwindings can be evaluated by means of the leakage factor, which is a constant that measures how much the short-circuit current is dispersed during a fault. The leakage factor depends on constructive aspects of the reactor, as the geometry of the windings and the physical dimensions of the reactor core. The leakage factor also depends on the percentage of turns involved, such that depending on the type of simulated fault (turn-to-ground fault or turn-to-turn fault) and the number of turns involved, the value of the leakage factor needs to be recalculated. In addition, the leakage factor should also be recalculated for each reactor specifically, depending on its constructive characteristics.

It should be noted that the value of the leakage factor varies between zero and one. When the leakage factor has values close to zero, the coupling between the subwindings is high and, consequently, the minimum leakage of fault current occurs, such that it presents higher values. On the other hand, when the leakage factor has a value close to one, the coupling between the subwindings is low and, consequently, the maximum leakage of fault current occurs, causing it to have low values.

In this sense, so that it is possible to make a comprehensive assessment of the leakage factor that encompasses extreme coupling situations, and considering the difficulty of finding such specific parameters of the reactor (such as its constructive aspects), the values defined and used in this article are: 0.25 (corresponding to a low value), 0.50 (corresponding to an intermediate value) and 1.00 (corresponding to corresponding to a high value). Thus, based on the adopted value of leakage factor and the number of turns involved in the fault, impedances of each subwinding (of the faulted phase) are calculated, which are used in the reactor model.

According to [17], for turn-to-ground faults, the faulted phase reactor winding is divided in two subwindings, n_f and n_g, coupled together in series. Thus, to carry out the parametric sensitivity analysis, the value of subwinding n_g is varied between 1% to 99% of turns of the faulty phase. The subwinding n_f is defined as $n_f = n_T - n_g$, where n_T is the total number of turns in the entire winding. Thus, the coupling between n_f and n_g is measured through the leakage factor α_{fg} for turn-to-ground faults.

Following the modeling described by [17], to carry out the turn-to-turn faults, the faulted phase winding must be divided into three subwindings coupled together in series: n_f, n_g and n_h. Thus, to execute the parametric sensitivity analysis, the subwinding n_f is fixed as being equal to 1% of turns of the faulted phase. For the subwinding n_g, the turns are varied between 1% to 98%. And finally, the subwinding n_h is defined as $n_h = n_T - n_f - n_g$. As for turn-to-turn faults the winding is divided into three parts, three leakage factors are defined (α_{fg}, α_{gh} and α_{fh}) and they measure the coupling between the three subwindings. It is noteworthy that, these three leakage factors is considered equal and labeled α_{tt} for the simulations of turn-to-turn faults.

The characteristics of turn-to-ground and turn-to-turn faults simulated in parametric sensitivity analysis are indicated in Tab. II. Furthermore, as turn-to-ground and turn-to-turn faults take only one of the phases, for these simulations the faults were always applied in phase A, in such way that only the performance of θ_A is presented.

TABLE II
FEATURES OF THE EVALUATED FAULTS FOR PARAMETRIC SENSITIVITY ANALYSIS.

Case	Type of Fault	Leakage Factor
8	Turn-to-ground	$\alpha_{fg} = 0.25$
9	Turn-to-ground	$\alpha_{fg} = 0.50$
10	Turn-to-ground	$\alpha_{fg} = 1.00$
11	Turn-to-turn	$\alpha_{tt} = 0.25$
12	Turn-to-turn	$\alpha_{tt} = 0.50$
13	Turn-to-turn	$\alpha_{tt} = 1.00$

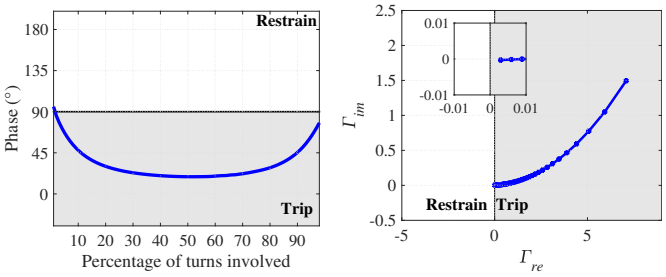

(a) (b)

Fig. 12. The performance for turn-to-ground faults with $\alpha_{fg} = 0.25$ of: (a) distance function (b) differential function.

As the differential protection function is not able to identify turn-to-ground and turn-to-turn faults with low fault current values, to carry out the comparative evaluation for the parametric sensitivity analysis, the performance of the algorithm reported in [6] is also presented. It is worth remembering that this algorithm corresponds to a differential function that operates based on the behavior of Γ, which is defined by the complex ratio between the zero sequence current and the neutral current of the reactor. The tripping occurs when the Γ indicator moves to the right left half-plane of the current alpha plane.

The results for turn-to-ground faults with $\alpha_{fg} = 0.25$ (that corresponds to Case 8 of Table II) are shown on Fig. 12. Note from Fig. 12(a) that θ_A shifts to the operating region for faults with more than 1% of turns short-circuited. The evaluated differential function operates independently of the number of turns involved, since Γ moved to the operation region for all simulated faults, as shown in Fig. 12(b).

For turn-to-ground faults with $\alpha_{fg} = 0.50$ (that corresponds to Case 9 of Table II), the results are presented on Fig. 13. It can be seen from Fig. 13(a) that θ_A shifts to the operating region for faults with more than 1% of turns short-circuited. The differential function operates independently of the number of turns involved, as shown in Fig. 13(b).

The results for turn-to-ground faults with $\alpha_{fg} = 1.00$ (that corresponds to Case 10 of Tab. II) are shown on Fig. 14. It is verified from Fig. 14(a) and Fig. 14(b) that both θ_A and independently of the number of turns involved.

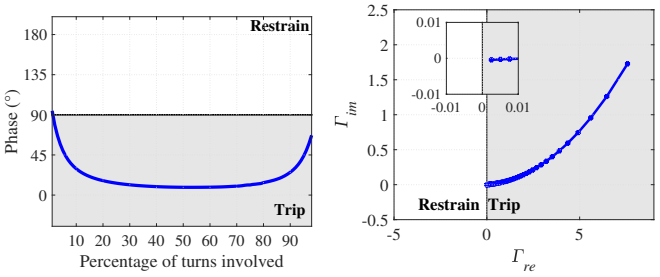

(a) (b)

Fig. 13. The performance for turn-to-ground faults with $\alpha_{fg} = 0.50$ of: (a) distance function (b) differential function.

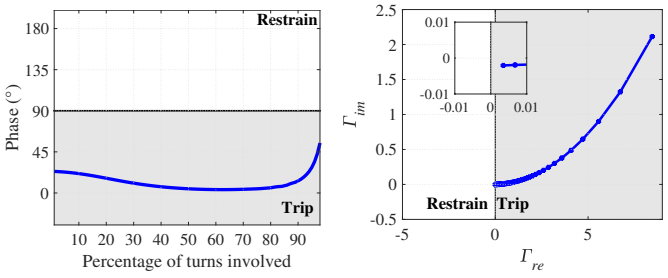

(a) (b)

Fig. 14. The performance for turn-to-ground faults with $\alpha_{fg} = 1.00$ of: (a) distance function (b) differential function.

For turn-to-turn faults with $\alpha_{tt} = 0.25$ (that corresponds to Case 11 of Tab. II), the results are presented on Fig. 15. It can be seen from Fig. 15(a) that θ_A shifts to the operating region for faults with more than 1% of turns short-circuited. The evaluated differential function operates independently of the number of turns involved, since Γ moved to the operation region for all simulated faults, as shown in Fig. 15(b).

The results for turn-to-turn faults with $\alpha_{tt} = 0.50$ (that corresponds to Case 12 of Table II) are shown on Fig. 16. Note from Fig. 16(a) that θ_A shifts to the operating region for faults with more than 1% of turns short-circuited. The differential function operates independently of the number of turns involved, as shown in Fig. 16(b).

For turn-to-turn faults with $\alpha_{tt} = 1.00$ (that corresponds to Case 13 of Table II), the results are presented on Fig. 17. It can be seen from Fig. 17(a) that θ_A shifts to the operating region only for faults with more than 13% of turns short-circuited. The evaluated differential function operates for faults with more than 15% of turns short-circuited, as shown in Fig. 17(b).

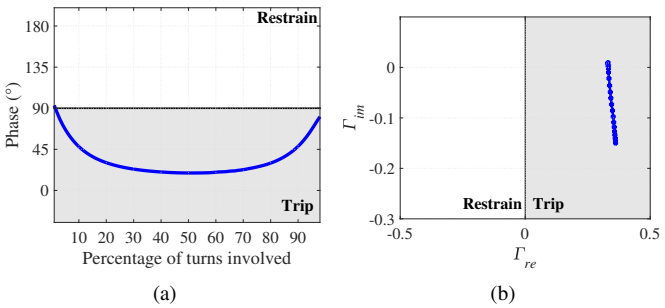

(a) (b)

Fig. 15. The performance for turn-to-turn faults with $\alpha_{tt} = 0.25$ of: (a) distance function (b) differential function.

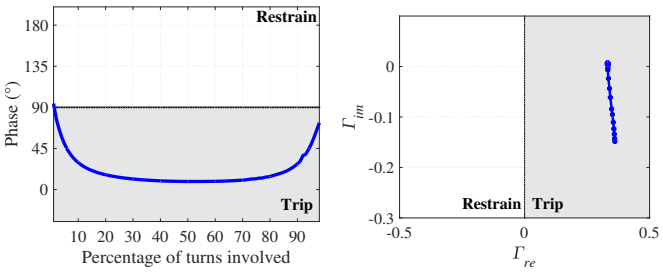

(a) (b)

Fig. 16. The performance for turn-to-turn faults with $\alpha_{tt} = 0.50$ of: (a) distance function (b) differential function.

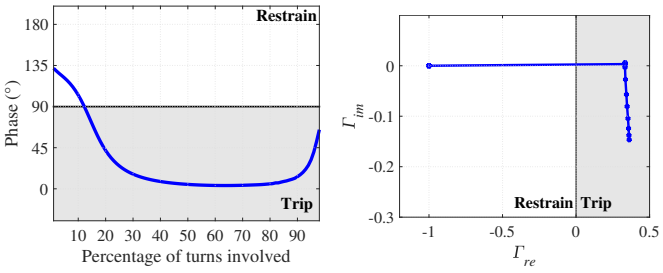

(a) (b)

Fig. 17. The performance for turn-to-turn faults with $\alpha_{tt} = 1.00$ of: (a) distance function (b) differential function.

IV. Discussion of Results

From the results obtained through the transient analyses, one can see that the distance protection function operates for phase-to-ground, phase-to-phase faults applied close to the phase terminals and with part of the winding short-circuited. Evaluating the performance of the differential function, it is verified that the faulted phases correctly moved to the tripping region, detecting the fault. It is noteworthy that, in fact, the differential protection function is normally used to identify those faults that result in high current. Comparing the performance of both distance and differential function the time, it is observed that they presented similar performance. Thus, distance function can be used together with the differential function to increase the secure of the protection scheme.

Based on the results obtained from the parametric sensitivity analysis, it is verified that the value of the leakage factor and the number of turns short-circuited little practically did not influence on the operation of the distance function. For most cases, the distance function operates for faults with more than 1% of short-circuited turns. Only for turn-to-turn faults with $\alpha_{tt} = 1.00$ the distance protection function detects the faults taking more than 14% of the turns short-circuited.

From the evaluated cases of external faults and energization, it can be verified that despite the oscillations caused by the transients, θ_ϕ was greater than 90°, such that the distance function does not operate, agreeing with theory indicated by Fig. 2(b). On the contrary, for internal faults, in most of cases θ_ϕ was smaller than 90°, such that the distance protection function operates, also being in accordance with the theory indicated by Fig. 2(a). It should also be noted that in the cases evaluated in the transient analysis, θ_ϕ had its value around 45°, which would guarantee safe operation, within the

mho characteristic and far from the operation threshold (which corresponds to the operation exactly at the circle indicated in Fig. 2, when $\theta_\phi = 90°$). The simulated cases in the parametric sensitivity analysis are also highlighted because they correspond to the most critical fault cases, due to the low fault currents, especially for faults with few short-circuited turns or with high leakage factor. For these cases, the value of θ_ϕ was close to $0°$ for most of the simulations, which would certainly guarantee safe operation of the distance protection function, within the mho characteristic and far from the operation threshold.

Based on the comparative evaluation between the distance and differential protection functions, it was observed once more they presented similar performance. However, it can be seen from the figures that show the performance of Γ for turn-to-ground and turn-to-turn faults that, despite moving to the operation region, Γ has small values: in the order of 10^{-3} for turn-to-ground faults and on the order of 10^{-1} for turn-to-turn faults. Depending on the accuracy of the equipment used in the protection system, these small values may not generate a trip, resulting in a failure in protection system operation. In this way, it is suggested the joint use of the distance function with the differential protection, because if the differential function does not operate, due to the small Γ values, the distance function would guarantee the operation, increasing reliability consequently.

In this sense, the distance and differential protection functions would be used together to protect the reactor. Indeed, if the differential protection function fails, the distance function is able to operate. It should be noted that for the implementation of the distance function for shunt reactors, the measurement of voltages made through the capacitive potential transformers (CPT) of the line was considered. Thus, additional measuring equipment would not be required. Moreover, the traditional differential function is already established, but it is not able to identify faults with small values. So the idea is to use the protection function reported in [6] in conjunction with the distance function.

V. Conclusions

From the results obtained through the simulations carried out in the ATP, it is stated that the distance protection identified the phase-to-ground and phase-to-phase faults simulated. It is also verified that the value of the leakage factor and the number of turns short-circuited little practically did not influence on the operation of the distance function. For most cases, distance function operate for faults with more than 1% of short-circuited turns for turn-to-ground and turn-to-turn faults.

In conclusion, considering the simulations carried out that employ a dry-type reactor and comparing the distance function and the differential function, it is verified that both protection functions presented similar performance, operating in the identification of critical faults with low value of fault current, such as turn-to-ground and turn-to-turn faults. These results can be used as a guide for further studies, for example, that evaluate the use of distance function to protect iron-core reactors, or for investigations that evaluate the influence of the leakage factor and the number of short-circuited turns on the performance of the distance function. Also, it is suggested the joint use of the distance function with the differential protection, increasing reliability of protection scheme for shunt reactors.

References

[1] G. Ziegler, *Numerical Differential Protection: Principles and Applications*, 2nd ed. Berlin: Siemens, 2012.

[2] B. Taj, A. Mahmoudi, and S. Kahourzade, "Comparison of low-impedance restricted earth fault protection in power- transformer numerical relays," *Australian Journal of Basic and Applied Sciences*, vol. 5, pp. 2458–2474, 12 2011.

[3] F. K. Basha and M. Thompson, "Practical EHV reactor protection," in *2013 66th Annual Conference for Protective Relay Engineers*, College Station, USA, 2013.

[4] "EMTP reference models for transmission line relay testing," IEEE Power System Relaying Committee), Tech. Rep., 2004.

[5] IEEE *Guide for the Protection of Shunt Reactors - Redline*, 2007, IEEE Std C37.109-2006 (Revision of IEEE Std C37.109-1988) - Redline.

[6] M. L. S. Almeida, L. M. Peres, and G. G. Santos, "Air-core dry-type shunt reactor protection based on an alternative current alpha plane," *IET Generation, Transmission & Distribution*, vol. 15, no. 1, pp. 34–44, 2021.

[7] R. G. Bainy and K. M. Silva, "Enhanced generalized alpha plane for numerical differential protection applications," *IEEE Transactions on Power Delivery*, vol. 36, no. 2, pp. 587–597, 2021.

[8] M. L. S. Almeida, L. M. Peres, and K. M. Silva, "On applying an enhanced generalized alpha plane to shunt reactor protection," *Electric Power Systems Research*, vol. 212, p. 108387, 2022. [Online]. Available: https://www.sciencedirect.com/science/article/pii/S0378779622005399

[9] CIGRE, "Protection, monitoring and control of shunt reactors," Working Group B5.37, Tech. Rep., 2012.

[10] K. Dobrzyński, Z. Lubosny, J. Klucznik, and S. Czapp, "Neutral earthing reactor protection," in *2017 IEEE International Conference on Environment and Electrical Engineering and 2017 IEEE Industrial and Commercial Power Systems Europe (EEEIC / I&CPS Europe)*, 2017, pp. 1–6.

[11] "Summary of the 'guide for the protection of shunt reactors' ansi c37.109," IEEE *Transactions on Power Delivery*, vol. 6, no. 1, pp. 116–118, 1991.

[12] Z. Gajić, B. Hillstrőm, and M. Kockott, *application of numerical relays for* HV *shunt reactor protection*, 2014.

[13] G. Ziegler, *Numerical distance protection: principles and applications*. John Wiley & Sons, 2011.

[14] Y. G. Paithankar, *Transmission network protection: theory and practice*. Routledge, 2017.

[15] K. Silva and M. Almeida, "Positive sequence voltage memory filter for numerical digital relaying applications," *Electronics Letters*, vol. 51, no. 21, pp. 1697–1699, 2015.

[16] *Modern Techniques for Protecting and Monitoring of Transmission Lines*, 2011, working Group B5.07: TB 465, Jun. 2011.

[17] P. Bastard, P. Bertrand, and M. Meunier, "A transformer model for winding fault studies," *IEEE Transactions on Power Delivery*, vol. 9, no. 2, pp. 690–699, 1994.